

# Passive decoy state quantum key distribution: Closing the gap to perfect sources

Wolfgang Maurer\* and Christine Silberhorn

Max-Planck Research Group for Optics, Information and Photonics, Junior Research Group IQO

(Dated: September 10, 2018)

We propose a quantum key distribution scheme which closely matches the performance of a perfect single photon source. It nearly attains the physical upper bound in terms of key generation rate and maximally achievable distance. Our scheme relies on a practical setup based on a parametric downconversion source and present-day, non-ideal photon-number detection. Arbitrary experimental imperfections which lead to bit errors are included. We select decoy states by classical post-processing. This allows to improve the effective signal statistics and achievable distance.

PACS numbers: 03.67.Dd, 03.67.Hk, 03.67.-a

Quantum key distribution (QKD) allows two parties (Alice and Bob) to communicate securely even in the presence of an arbitrarily powerful eavesdropper (Eve) who tries to listen undetected. To prove unconditional security, Eve must not be restricted by any technological limitations, but must only be bounded by the laws of quantum physics. A multitude of protocols has been suggested in the last decades; BB84 [1] is the best-known and usually best-performing protocol. It was shown to be secure both in principle, [2] and references therein, and in the presence of experimental imperfections, *e.g.*, [3]. Unfortunately, the maximal distance and the bit rates over which secure communications can be guaranteed are strongly constricted if experimental imperfections are taken into account: lossy channels, imperfect detectors with finite efficiency, dark counts and misalignment errors, as well as non-ideal signal sources – which do not provide the required single photon states [4, 5] – degrade the performance of the protocol. Decoy-state QKD, which was recently introduced by [6], analyzed in [7, 8] and adapted for practical use in [9, 10], could mend this. Still, coherent state implementations achieve only about 70% of the maximal secure distance imposed by fundamental physics.

In this paper, we show how we can close the gap between practical QKD implemented with state-of-the-art devices and idealized QKD assuming perfect single-photon signals. In our approach, a parametric downconversion (PDC) source [11] in conjunction with a photon number resolving detector [12] – as depicted in Fig. 1 – is utilized to implement a passive decoy-state QKD scheme. It does not require any active intensity modulation, but allows to improve the effectively sent signal statistics by employing conjugate PDC modes. Strict photon-number correlations between the two PDC outputs allow to infer the complete statistical information about one of them by measuring the photon number distribution of the other. Passive data analysis enables us to generate optimized effective signal statistics without physical blocking. For all practical purposes, our protocol accomplishes up to few percent the power of a single photon source in terms of distance, while the key generation rate is on par with

the best available schemes.

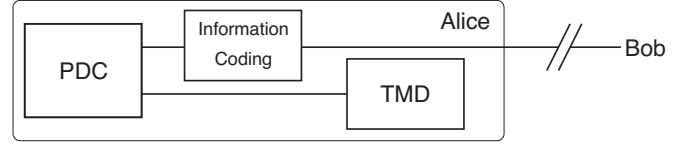


FIG. 1: Setup of the proposed QKD scheme. The PDC source emits photon-number correlated bipartite states; the TMD records photon statistics.

Since our work is based on the decoy state method, we begin by briefly reviewing the basic idea. The security of BB84 relies on single photons, so signals with more than one photon are insecure because Eve can perform a photon-number splitting (PNS) attack, which has been shown to be optimal [13]. For this, Eve performs a quantum non-demolition measurement of the photon number, taps one photon and delays the measurement until Alice and Bob announce the bases. If Eve replaces the lossy channel with a perfect one and passes on the same statistics as in the lossy channel, this attack can not be detected in a standard BB84 scheme. The probability that at least one photon of an  $n$ -photon signal passes a quantum channel with transmission  $\eta = \exp(-\alpha/10 \cdot l)$  (where  $\alpha$  is the loss in dB/km and  $l$  is the channel length in km) is given by  $\eta_n = 1 - (1 - \eta)^n$ , different loss characteristics arise for signals with different photon numbers. The core idea of the decoy method is to check that the signal losses behave as expected for different photon numbers to exclude PNS attacks. For this, it is necessary to intersperse the signal stream with decoy states whose intensity differs slightly from the signal states, but share all other characteristics like wavelength and timing. A more detailed description can be found in the work of Lo and coworkers [7].

The security analysis in [7] proofs that a lower bound on the secure key generation rate is given by

$$\begin{aligned} S' &= q\{-Q_x f(E_x) H_2(E_x) + Q_1 \cdot (1 - H_2(e_1))\}, \\ S &\geq S' \cdot \Theta(S'). \end{aligned} \quad (1)$$

In Eqn 1 the *gain*  $Q_\chi$  denotes the ratio of Bob's detection events to Alice's number of submitted signals after sifting; the *yield*  $Y_n$  is defined as the probability that Bob receives a signal conditioned on that Alice has sent an  $n$ -photon signal. The parameters  $E_\chi$  and  $e_n$  describe the overall, and the photon number resolved quantum bit error rate (QBER), *i.e.*, the fraction of signals which contribute false key bits although a signal was received. The quantities are related as follows:

$$Q_\chi \equiv \sum_{n=0}^{\infty} Q_n = \sum_{n=0}^{\infty} Y_n p(n), \quad (2)$$

$$E_\chi Q_\chi \equiv \sum_{n=0}^{\infty} Y_n p(n) e_n. \quad (3)$$

The function  $f(x)$  in Eqn. 1 accounts for non-ideal practical error correction which does not reach the Shannon limit, and  $H_2(x)$  is the binary Shannon entropy. The sifting factor  $q$  corrects incompatible bases, *i.e.*, for standard BB84  $q = 1/2$ . In the asymptotic limit it is possible to reach values of  $q \approx 1$  [5], this is used in the remainder of the paper. Conventional QKD schemes employ binary detectors. Thus, only the overall gain  $Q_\chi$  and QBER  $E_\chi$  can be measured during transmission. Source characterization guarantees that  $p(n)$  is known. The decoy state idea exploits that the linear system of Equations (2) and (3) can be solved for  $Y_n$  and  $e_n$ , if states with different mean intensities are employed. While  $Y_n$  and  $e_n$  are identical in Eve's absence for the signal and all decoy states, it is proven that any PNS attack will modify these quantities, *i.e.*, Eve's attempt of an PNS attack will be detected [7].

The original security proof for BB84 given in [14] utilized local operations and one-way classical communication (1-LOCC). While many security analyses retain with 1-LOCC, enhanced security proofs employing 2-LOCC [2] have been elaborated recently and adapted to the decoy method in [15]. Two-way postprocessing is performed by comparing parities for random bit pairs in Alice's and Bob's key. If the parities match, they keep the first bit, otherwise they discard both. One round of this procedure is called a B-step; repeating it for several rounds is possible and allows to increase the maximal secure distance. For comparison we consider both cases, 1-LOCC and 2-LOCC.

Consider the setup in Fig. 1. In the source, we use a standard PDC process to obtain the photon-number correlated state

$$|\psi\rangle = \frac{1}{\mathcal{N}} \sum_{n=0}^{\infty} \lambda_n |n, n\rangle, \quad (4)$$

where  $\lambda$  and the normalization factor  $\mathcal{N}$  depend on the physical boundary conditions [16]. The distribution exhibits Poissonian ( $\lambda_n = \frac{\lambda^n}{n!}$ ,  $\mathcal{N} = e^{-\lambda^2}$  [26]) or thermal

( $\lambda_n = \tanh^{2n} \chi$ ,  $\mathcal{N} = \cosh^2 \chi$ ) statistics in the extremal cases, so we will consider both possibilities. Since Eve has no phase reference, the phase is assumed to be totally randomized, and an effective mixture of photon number eigenstates with density operator  $\varrho = \sum_n |\lambda_n / \mathcal{N}|^2 \varrho_n$  is transmitted.

Information encoding can be accomplished by polarization or time coding, but the exact method is of no relevance for the further analysis. A time multiplexed detector (TMD) provides photon number resolution capabilities. There are several methods to perform photon number resolution, but we focus on TMD detection [12] since it is cost-effective and easy to handle experimentally. The measured TMD statistics can be related to the impinging photon number statistics by

$$\vec{p}_{\text{source}} = \mathbf{L}^{-1} \cdot \mathbf{C}^{-1} \cdot \vec{p}_{\text{meas}} \equiv \mathcal{R}(\vec{p}_{\text{meas}}) \quad (5)$$

where the loss matrix  $\mathbf{L}$  accounts for photon loss in the detection, and the convolution matrix  $\mathbf{C}$  models the effect of a finite number of detected modes in the TMD design (for details: see [12]);  $\vec{p}_s$  and  $\vec{p}_m$  describe the original photon number distribution of the source and the measured statistics. The quantity  $\mathbf{C} \cdot \mathbf{L}$  can be determined by measurement, but there is also an analytical representation  $p_\eta(m|n)$  for the matrix entries given in [17]. It represents the probability to get an  $m$ -photon detection outcome conditioned on  $n$  photons entering the detector with total loss  $\eta$ . Using Eqn. 5, the TMD measurement can be inverted so that the real statistics of the source are reconstructed with high fidelity [18]. Note that this inversion is only possible for an ensemble of states, but not for a single signal, so Alice needs to record the measurement results of the TMD for every time slot. After this, Alice and Bob follow the standard protocol of BB84 [4] for information encoding and analysis.

The essential step of passive decoy state selection follows after a sufficiently large number of signals (say,  $N_{\text{tot}} \gg 1$ ) has been transmitted; note that Alice will run the source with constant pump intensity and without any active optical manipulations for the duration of the procedure. Fig. 2 provides an overview about the process: The measured discrete probability distribution  $\vec{p}_{\text{meas}}$  is calculated by  $p_{\text{meas}}(n) = \frac{\#n_{\text{tot}}}{N_{\text{tot}}}$ , where  $\#n_{\text{tot}}$  denotes the number of  $n$ -photon measurement outcomes from the TMD. This distribution can be inverted by Eqn. 5; the strict photon number correlations of the PDC states ensure that Alice's measurement coincide with the signal statistics.

Assume that we start with a random selection of a set containing  $M \ll N_{\text{tot}}$  signals to construct decoy states, which have exactly the same statistics as the remaining signal states. Alice then additionally picks  $\delta_n$  slots with an  $n$ -photon measurement result such that

$$\#n_{\text{decoy}} = \#n_{\text{tot}} \cdot \frac{M}{N_{\text{tot}}} + \delta_n \quad (6)$$

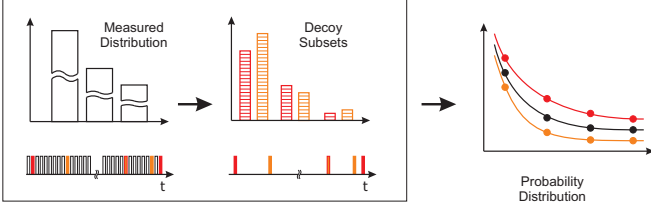


FIG. 2: (Color online) Classical decoy state selection. A part subsets of the recorded TMD measurements are selected and inverted to form the decoy states which are similar to the signal state. The photon number distributions are not drawn to scale for instructive purposes.

where  $\delta_n$  is a small positive or negative offset which results in a photon number distribution of the decoy subset differing slightly from the distribution in the signal. The decoy subset can be inverted to obtain the proper probability distribution  $\vec{p}_{\text{decoy}}$ . Depending on how many decoy states are to be used (one vacuum state and two decoy states similar to the signal are sufficient, cf. [9, 19]), an appropriate number of subsets has to be chosen. Different distributions of  $\delta_n$  for different subsets ensure that the generated decoy signals are sufficiently distinct from each other as required to solve the system of linear equations (2,3). We would like to stress that our passive method for “generating” decoys provides distinct advantages: during signal transmission it is still undecided which states will become signal or decoy states. This implies that a distinction between signal and decoy states by Eve is not possible, even in principle. It is also important to emphasize that our decoy selection mechanism eliminates many experimental challenges (*e.g.*, different spectra of the generated PDC light for signal and decoys which gives Eve a chance to experimentally distinguish between them) which arise in proposals with the same hardware, but a different analysis procedure ([20, 21]), which do not draw maximal use of the TMD’s capabilities. The remainder of the protocol is identical to a standard decoy scheme: Alice and Bob check  $e_n$  and  $Y_n$  as described above. Error correction and privacy amplification need to be performed to generate a final secure key. The inset in Fig. 3 presents our simulation results (for details see below). The key generation rate and maximal secure distance closely match a perfect single photon source.

The TMD results can not only be used to generate decoy states, but also provide improved effective signal statistics. While the error rates  $e_n$  for  $n \geq 1$  are the order of  $10^{-2}$ , the contribution by vacuum signals is  $e_0 = 1/2$  [27]. Thus, it is desirable to remove such events as good as possible. Decreasing the dark count rate on Bob’s side is hard because it requires refinement of the detectors, while fine-grained time triggering can be used on Alice’s side to reduce the dark count probability in the TMD to a negligible level, *i.e.*,  $p(n|m) = 0$  for  $n > m$  [12].

Note that due to losses and imperfect detection, filtering multi-photon contributions does not work perfectly and results in comparatively small rate improvements ([20]). The benefits are negligible in contrast to filtering zero photon contributions. Alice has recorded the TMD measurement for every signal. Hence she can easily discard all zero events in the postprocessing phase which leads to a better effective probability distribution given by

$$p_{f,\text{meas}}(n) = \begin{cases} 0 & n = 0 \\ \frac{1}{N_{\text{tot}} - \sum_{n=1}^{\infty} \#n} \cdot \frac{\#n}{N_{\text{tot}}} & n \geq 1 \end{cases}, \quad (7)$$

where  $p_{f,\text{meas}}$  denotes the measured, filtered distribution; the effectively sent distribution is  $\vec{p} = \mathcal{R}(\vec{p}_{f,\text{meas}})$ . Since  $p(0|n) \neq 0$  for  $n > 0$ , some usable signal states are also removed from the distribution, but this does not endanger the total positive effect of the filtering. To implement the operation, Alice and Bob need to discard all slots in the postprocessing stage where the TMD result was zero and use the inverted probability distribution in the rate calculations.

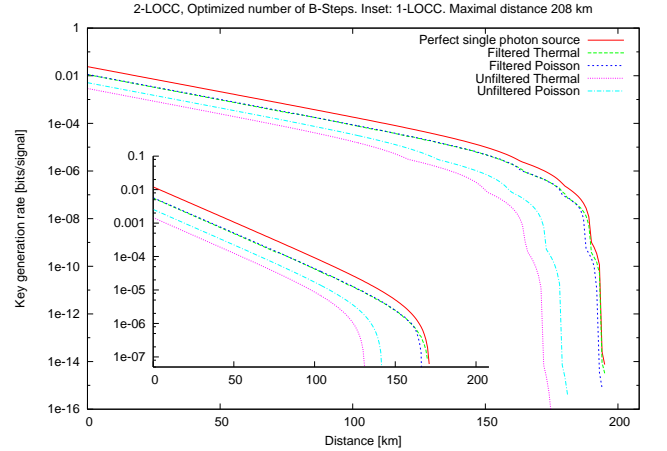


FIG. 3: (Color online) Simulation results for two-way and one-way (inset) classical communication. Both graphs were obtained by a numerical evaluation of Eqn. 1; the optimal values for  $\chi$  and the number of B-Steps which maximize the key generation rate have been used for all distances. The right border represents the principal upper bound given by the intercept-resend attack.

Note that filtering of this type does not reduce the signal rate: A subset of the signal set is removed during postprocessing because this subset will make the overall result only worse. No physical blocking of signals is performed. This leaves the transmitted signals unmodified. Fig. 3 and Tab. I present the results of the numerical evaluation for all cases discussed above: Signals with and without filtering for both 1- and 2-LOCC. Note that we apply an optimization for both, the best value for  $\chi$  and the ideal number of B-Steps for every distance. To allow comparison with other proposals, we use the set of experimental parameters given in [22]. The upper

bound on the secure distance caused by the undetectable intercept-resend attack at a QBER of more than 25% [5] lies at 208km, *i.e.*, the right border of the graph. The *lower* bound on our rate closely approaches this *upper* limit, and reaches the single photon performance. One also needs to keep in mind that this upper bound is not even tight, but can be replaced by smaller ones (*e.g.*, [23]).

The filtering transformation in Eqn. 7 modifies the effective signal distribution so that a different rate is obtained although the sent statistics remain unmodified. Thus, a penalty factor needs to be introduced into Eqn. 1 when an optimal  $\chi$  is sought to maximize  $S$ :  $S \geq p_{\text{pen}} \cdot S' \cdot \Theta(S')$ ,  $p_{\text{pen}} = 1 - \sum_{n=0}^{\infty} p(0|n)p_s(n)$ . The optimal values for  $\chi$  depend on the simulation parameters and the source statistics; a comprehensive set of results for different combinations can be found in [24]. Here it suffices to know that the range for  $\chi$  is (0, 0.5) which can well be realized with current PDC sources [25]. Existing sources provide better performance than actually required.

| Source             | distance<br>unf./filt. | $\Delta_{1,f}$ | $\Delta_{2,f}$ |
|--------------------|------------------------|----------------|----------------|
| Thermal (1-way)    | 130.8/169.7            | 0.7%           | 18.3%          |
| Thermal (2-way)    | 174.5/194.5            | 0.4%           | 6.3%           |
| Poissonian (1-way) | 141.2/166.0            | 2.9%           | 20.0%          |
| Poissonian (2-way) | 180.8/193.8            | 0.7%           | 6.6%           |

TABLE I: Comparison of the obtainable distances for different signal sources and postprocessing methods with the limits set by a perfect single photon source and the principal physical upper bound. A perfect single photon source achieves 170.9km for 1-LOCC and 195.2km for 2-LOCC.  $\Delta_{1,f}$  denotes the difference to this distance.  $\Delta_{2,f}$  denotes the the difference to the principal intercept-resend upper bound. Both refer to the effectively filtered source. At most 4 B-Steps were used.

As explained above, two-way processing with B-steps can increase the achievable distances. Ma *et al.* [15] calculated that after performing a B-Step, a lower bound on the secure key generation rate is given by  $S' = qQ_{\chi} (\frac{1}{2}s_{n \neq 1} (-f(E'_{\chi})H_2(E'_{\chi}) + \Omega'(1 - H_2(e'_{1,p}))))$ ,  $S \geq S' \cdot \Theta(S')$ . A detailed derivation of the formula is beyond the scope of this paper, but can be found in Refs. [15, 24]. Multiple rounds of B-Steps apply the transformation multiple times). The difference between the lower bound on the maximal secure distance and the principal limit shrinks to about 6.5% with 4 B-Steps as shown in Tab. I.

In summary, we have shown how to use the photon number correlations of a PDC source to implement a BB84 scheme which nearly reaches the performance of a single photon scheme. This removes the predominant imperfection from real-world QKD implementations. Since the lower bound on the key generation rate coincides up to a few percent with the principal upper bounds, fur-

ther improvements need either come from new protocols or improved hardware. Refinements of security proofs will likely be unfruitful by comparison.

We acknowledge helpful comments by N. Lütkenhaus, H.-K. Lo and J. Lundeen.

---

\* Electronic address: wolfgang.mauerer@ioip.mpg.de

- [1] C. H. Bennet and G. Brassard, in *Proc. IEEE Int. Conf. Comp., Syst., and Sig.* (1984), pp. 175–179.
- [2] D. Gottesman and H.-K. Lo, *IEEE Transactions on Information Theory* **49**, 457 (2003).
- [3] D. Gottesman, H.-K. Lo, N. Lütkenhaus, and J. Preskill, *Quant. Inf. & Comp.* **4**, 325 (2004).
- [4] N. Gisin, G. Ribordy, W. Tittel, and H. Zbinden, *Rev. Mod. Phys.* **74**, 145 (2002).
- [5] M. Dušek, N. Lütkenhaus, and M. Hendrych, To appear in *Progress in Optics* (2006).
- [6] W.-Y. Hwang, *Phys. Rev. Lett.* **91**, 057901 (2003).
- [7] H.-K. Lo, X. Ma, and K. Chen, *Phys. Rev. Lett.* **94**, 230504 (2005).
- [8] X. B. Wang, *Phys. Rev. Lett.* **94**, 230503 (2005).
- [9] J. W. Harrington, J. M. Ettinger, R. J. Hughes, and J. E. Nordholt, *arXiv:quant-ph/0503002* (2005).
- [10] X. B. Wang, *Phys. Rev. A* **72**, 049908 (2005).
- [11] L. Mandel and E. Wolf, *Optical Coherence and Quantum Optics* (Springer, 1995).
- [12] D. Achilles, C. Silberhorn, C. Sliwa, K. Banaszek, and I. A. Walmsley, *Opt. Lett.* **28**, 2387 (2003).
- [13] N. Lütkenhaus and M. Jähma, *New Journal of Physics* **4**, 44.1 (2002).
- [14] P. W. Shor and J. Preskill, *Phys. Rev. Lett.* **85**, 000441 (2000).
- [15] X. Ma, C.-H. F. Fung, F. Dupuis, K. Chen, K. Tamaki, and H.-K. Lo, *arXiv:quant-ph/0604094* (2006).
- [16] J. Perina Jr, O. Haderka, and M. Hamar, *arXiv:quant-ph/0310065* (2003).
- [17] M. J. Fitch, B. C. Jacobs, T. B. Pittman, and J. D. Franson, *Phys. Rev. A* **68**, 043814 (2003).
- [18] D. Achilles, C. Silberhorn, and I. A. Walmsley, *Phys. Rev. Lett.* **97**, 043602 (2006).
- [19] X. Ma, B. Qi, Y. Zhao, and H.-K. Lo, *Phys. Rev. A* **72**, 012326 (2005).
- [20] T. Horikiri and T. Kobayashi, *Phys. Rev. A* **73**, 032331 (2006).
- [21] Q. Y. Cai and Y. G. Tan, *Phys. Rev. A* **73**, 032305 (2006).
- [22] D. Gobby, Z. Yuan, and A. Shields, *Appl. Phys. Lett.* **84**, 19 (2004).
- [23] T. Moroder, M. Curty, and N. Lütkenhaus, *Phys. Rev. A* **73**, 012311 (2006).
- [24] W. Mauerer and C. Silberhorn, *Manuscript in preparation* (2006).
- [25] A. B. U'Ren, C. Silberhorn, K. Banaszek, and I. A. Walmsley, *Phys. Rev. Lett.* **93**, 093601 (2004).
- [26]  $\chi$  is a coupling strength and interaction time parameter; the mean photon number is given by  $\sinh^2 \chi$  [11].
- [27] If a vacuum pulse is sent and a dark count causes one detector to click, it is the wrong one with 50% chance.